Version of Record: https://www.sciencedirect.com/science/article/pii/S0959652618333092
Manuscript_0d43962049f25fc72de6550d8f7f81bd

Continuous Condensed-Phase Ethanol Conversion to Higher Alcohols: Experimental Results and Techno-Economic Analysis

Iman Nezam, Lars Peereboom, and Dennis J. Miller
Department of Chemical Engineering and Materials Science
Room 2100 Engineering Building, 428 South Shaw Lane
Michigan State University
East Lansing, Michigan 48824 U.S.A
nezamima@msu.edu, peereboo@msu.edu, millerd@egr.msu.edu

Abstract

The conversion of ethanol to n-butanol and higher alcohols is carried out in a continuous fixed bed reactor over a $Ni/La_2O_3/\gamma\text{-}Al_2O_3$ catalyst at 210-250 ^oC and 100 bar. At these conditions, the reaction mixture is a condensed, near-critical phase that facilitates higher reaction rates than corresponding vapor phase reactions. Combined selectivity to n-butanol and C_6+ higher alcohols reached 74% at 41% ethanol conversion. A process concept is presented in which n-butanol and mixed C_6+ alcohols are produced as saleable products; ethanol is recycled to achieve nearly 100% overall conversion and minor byproducts are burned to provide process energy. A process design is conducted using Aspen Plus V8.4 process simulation software, and economic analyses are carried out for several cases of ethanol conversion and alcohol selectivities. Several additional cases involving permutations of the base process configuration are also examined in attempts to improve process economics. At n-butanol selectivities achieved experimentally, a facility producing 75 million kg n-butanol per year has a total capital cost of $38.1 million with a required n-butanol selling price of $1.55/kg to $1.60/kg for typical values of expected return on investment.

Keywords: Ethanol conversion, n-butanol, catalysis, process, economic analysis

Declaration of Interest: none

[1]To whom correspondence should be addressed at the above address. Email: millerd@egr.msu.edu; Voice: (517) 353-3928; Fax (517) 432-1106

Text word count: 7295

© 2018 published by Elsevier. This manuscript is made available under the Elsevier user license
https://www.elsevier.com/open-access/userlicense/1.0/

1. Introduction

The production of bioethanol from plant carbohydrates has been a major achievement in the ongoing challenge of finding alternatives to fossil fuels (Nagy, 2007; Sánchez and Cardona, 2008). However, ethanol has significant limitations as a biofuel for blending with gasoline, including low energy density, water absorption in high concentrations, and as yet high costs from cellulosic feed stocks. In contrast, n-butanol (C_4H_9OH) as a biofuel alleviates many of the problems associated with petroleum blending: it has 20% higher energy density and limited miscibility with and affinity for water. In addition, n-butanol is used as a large-scale commodity chemical and has a wide range of applications in industries such as paints and coatings, solvent and ester production, and cosmetics and pharmaceuticals (Ndaba et al., 2015; Nezam et al., 2017). Thus, efficient production of n-butanol in the biorefinery would enhance the economic viability of replacing petroleum resources with bio-based feed stocks.

Butanol is currently produced from petroleum by the "oxo" process (propene hydroformylation followed by hydrogenation) (Uyttebroek et al., 2015). From renewable biomass materials, n-butanol can be produced along with acetone and ethanol (ABE) by fermentation using *Acetobutylicum* bacteria (Algayyim et al., 2018; Patakova et al., 2013). Low productivity and high recovery costs (Pfromm et al., 2010) with *Acetobutylicum* have led to fermentation with modified *Clostridium* strains (Khamaiseh et al., 2014) that give higher n-butanol production rates. Further process improvements have been made through the use of recovery methods integrated with fermentation (Green, 2011; Lodi et al., 2018; Staggs and Nielsen, 2015). Despite these advances, the challenges of low titer, high separation costs, and overall ABE yield remain barriers for n-butanol fermentation systems (Algayyim et al., 2018).

n-Butanol and higher alcohols can also be produced via condensation of ethanol. First introduced by Marcel Guerbet in 1909, the set of reactions to produce butanol and higher alcohols from ethanol (and other alcohols) are called Guerbet reactions (De Gennes, 1909). The availability of bioethanol is a major motivation for butanol production via this route (Gabriëls et al., 2015). Two possible reaction mechanisms for Guerbet reactions have been proposed: direct condensation of the alcohols (Chieregato et al., 2015; Ndou et al., 2003; Yang and Meng, 1993), and the more generally accepted three-step mechanism involving dehydrogenation, aldol condensation, and hydrogenation reactions. The latter is especially favored at lower reaction temperatures and over metal-containing catalysts (Gabriëls et al., 2015; Jordison et al., 2016, 2015). Figure 1 shows the three-step aldol condensation mechanism leading to the production of butanol and higher alcohols (C_6+) from ethanol.

Several heterogeneous and homogeneous catalytic systems have been proposed for the Guerbet reactions. Heterogeneous catalysts are generally preferred due to lower separation costs and fewer environmental difficulties (Gabriëls et al., 2015; Wu et al., 2018). Chief among

these catalysts are MgO (Kozlowski and Davis, 2013; Ndou et al., 2003; Olson et al., 2004), multi-metal mixed oxides (Hernández et al., 2016; Marcu et al., 2013; Silvester et al., 2017), hydroxyapatite (Ho et al., 2016; Ogo et al., 2011; Scalbert et al., 2014; Tsuchida et al., 2008), alkali exchanged zeolites (Yang and Meng, 1993; Yoshioka et al., 2015), and alkaline activated carbon-supported catalysts (Onyestyák, 2018; Onyestyák et al., 2017). While most studies have failed to exceed a C_4+ alcohol selectivity of 75% with ethanol conversions above 40%, there is consensus that an ideal acid-base balance is the key to the desired catalyst activity and higher alcohols selectivity.

Nickel metal supported on alumina has been recently introduced for the Guerbet reaction (Ghaziaskar and Xu, 2013; Riittonen et al., 2015, 2012). A significant property of this catalyst is its activity at lower temperatures (<250 ^{o}C), which not only allows the reaction to be run in the condensed phase at elevated pressures, but also slows ethanol decomposition to undesired gaseous products such as CO_2 and CH_4. Jordison (Jordison et al., 2016, 2015) further improved conversion and selectivity of Ni/γ-Al_2O_3 by adding La_2O_3 onto the support. This modified catalyst gave a higher alcohol selectivity of 71% at an ethanol conversion of 55% in a stirred autoclave reactor at 230 ^{o}C and autogenous pressures.

In addition to studies of catalyst performance, a series of papers have been published (Dias et al., 2014; Pereira et al., 2014; Pereira et al., 2015a; Pereira et al., 2015b) that compare economics and environmental impacts of n-butanol formation from ethanol via the Guerbet reaction with n-butanol formation via the traditional petroleum-based “oxo” route (Pereira et al., 2015a) and with n-butanol production via ABE fermentation. Feed stocks examined for ABE fermentation include Brazilian sugar cane (Pereira et al., 2015b; Väisänen et al., 2016), corn grain (Brito and Martins, 2017; Tao et al., 2014; Väisänen et al., 2016), corn stover (Tao et al., 2014), wheat straw (Brito and Martins, 2017), Canadian pulp pre-hydrolysate (Levasseur et al., 2017), and others (Quiroz-Ramírez et al., 2017).

In the above studies, n-butanol production from ethanol is integrated into the biorefinery, and the overall economics and environmental impacts of the integrated refinery are reported. Two scenarios for Guerbet reactions are examined: vapor phase reaction at high temperature and low pressure as proposed by Tsuchida et al. (Tsuchida et al., 2008, 2006), and condensed phase reaction at lower temperature and elevated pressure (Riittonen et al., 2012). These studies make several assumptions regarding reaction rates, catalyst stability, and byproduct purification that have significant effects on the overall economic and environmental impacts from the different processes. Because n-butanol production is integrated into the overall ethanol biorefinery, it is difficult to gain a realistic assessment of the environmental impact or economic potential related specifically to n-butanol production. The economics of producing 2-ethylhexanol from ethanol via Guerbet reactions has also been examined (Patel et al., 2015), but yields used in the analysis do not reflect available experimental values so the validity of the analysis is uncertain.

In this work, we describe experiments and the economic analysis of a continuous condensed-phase stand-alone process for the production of n-butanol and higher alcohols using ethanol as feed stock. The process includes an improved distillation concept to purify n-butanol, and produces a mixed C_6+ alcohols stream as a byproduct instead of separating out individual minor products formed. Several alternate process configurations are evaluated as well in order to better ascertain the required selling price of n-butanol from ethanol. The economic analysis for each process configuration investigation is based upon a rigorous Aspen Plus V8.4 simulation using the S-R Polar equation of state from our prior work (Jordison et al., 2016).

2. Materials and Methods

2.1 Materials and catalyst preparation

Anhydrous ethanol (Koptec, 200 proof) was used as the feed in all experiments. $Ni(NO_3)_2 \cdot 6H_2O$ (99.999%, Aldrich), and $La(NO_3)_3 \cdot 6H_2O$ (>99%, Fluka) were used as catalyst precursors and spherical 1.6 mm diameter γ-Al_2O_3 (Strem Chemical) was used as the catalyst support. Two catalysts were prepared for this study: 8 wt% Ni/4.5 wt% La_2O_3/γ-Al_2O_3 and 1 wt% Ni/9 wt% La_2O_3/γ-Al_2O_3.

Catalysts were prepared using incipient wetness impregnation according to prior work (Jordison et al, 2015, 2016). To the alumina support, La_2O_3 was first impregnated by adding $La(NO_3)_3$ solution containing the desired quantity of lanthanum to the support in a quantity equal to the support pore volume, followed by drying at 130 ^oC for 20 h and calcination at 600 ^oC for 18 h in 50 mL/min N_2, to ensure the presence of La_2O_3 on the support surface. The same process was used for the addition of Ni (as $Ni(NO_3)_2 \cdot 6H_2O$) to the La_2O_3/γ-Al_2O_3 support, with an additional step of NiO reduction to Ni at 520 ^oC for 18 h using 50 mL/min H_2 at 1 atm.

2.2 Reactor system

Reactions were performed in a 1.91 cm OD (1.57 cm ID) x 76 cm length jacketed stainless steel up-flow packed bed reactor with a 3 mm OD internal thermowell to measure the temperature profile in the reactor during reaction. The reactor was heated with silicon oil using a Julabo (Model SE-6) heating circulator, with the reaction temperature ranging from 210 ^oC to 250 ^oC. Silicon carbide (SiC, 20-50 mesh) was packed in the reactor inlet for preheating the feed, and stainless steel rod fillers were used on the top and bottom of the reactor to reduce the dead space inside the reactor. Figure 2 shows a schematic of the reactor system.

Typically, 35 g of SiC and 30 g of catalyst supported on a quartz wool plug were placed in the reactor. The reactor was assembled and connected to the oil bath, and hydrogen gas was passed through the catalyst for 90 minutes after it reached the desired temperature to reduce surface nickel oxidized by exposure to air. A Bio-Rad (Model 1350) liquid chromatography pump was used for dispensing liquid ethanol feed to the reactor. Liquid flow rates varied from 0.5 mL/min to 1.3 mL/min, corresponding to a weight hourly space velocity (WHSV) of 0.8 – 2.1 kg ethanol/kg catalyst/h. A pressure relief valve was connected to the reactor outlet. The reactor

effluent was cooled to ambient temperature in a double pipe heat exchanger using building water as the coolant. A Tescom (Model 26-1764-24) back pressure regulator was used to control reactor pressure at 100 bar and reduce the effluent pressure to near atmospheric. Following pressure reduction, condensable products were recovered in collection vessels submerged in an ice bath (0 ^{o}C), and gaseous products that passed through the collection vessels were collected periodically in gas bags. Steady state was assumed to be achieved after 6-8 residence times of feed materials through the reactor.

2.3 Analytical Methods

Liquid product samples were diluted 10-fold in acetonitrile and analyzed using a Varian 450 gas chromatograph (GC) with flame ionization detector. A 30 m SolGel-Wax column (0.53 mm ID, 1 μm film thickness) was used with the following temperature program: initial temperature 37 ^{o}C for 4 min; ramp at 10 ^{o}C/min to 90 ^{o}C, and hold at 90 ^{o}C for 3 min; ramp at 10 ^{o}C/min to 150 ^{o}C; ramp at 30^{o}C/min to 230^{o}C and hold for 2 min. Butyl hexanoate was used as an internal standard to improve the precision of the analytical calculations. Gas samples were analyzed using a Varian 3300 GC with a thermal conductivity detector. A 4.57 m × 1.25 mm SS 60/80 Carboxen 1000 column (2.1 mm ID) was used with the following temperature program: initial temperature 35 ^{o}C for 5 min, then ramp at 20 ^{o}C/min to 225 ^{o}C.

The concentration of each species in the product mix was determined using response factors obtained from multi-point calibration curves. Response factors for unidentified components appearing in the chromatogram were taken as average values for species in close proximity to unidentified components. The calculated concentrations were entered into an in-house Excel spreadsheet to calculate ethanol conversion, product selectivity (mol ethanol to product/mol ethanol converted), product yield (mol ethanol to product/mol ethanol fed), and overall carbon recovery.

3. Experimental Results

Control experiments with only γ-Al_2O_3 support or La_2O_3/γ-Al_2O_3 gave less than 2% ethanol conversion and less than 20% selectivity to desired condensation products, an indication that the support alone is inactive, and that Ni plays a key role in Guerbet reactions.

Representative results of steady state experiments in the fixed bed reactor for two Ni-based catalysts are reported in Table 1. The 1 wt% Ni catalyst shows lower conversion than the 8 wt% Ni material, but less gas and liquid byproduct formation and overall higher selectivity to higher alcohol products. For each catalyst, as temperature increases or as space velocity decreases, ethanol conversion increases, selectivity to higher alcohols (n-butanol + C_6+ alcohols) declines, and the quantity of gas and liquid byproducts formed increases. Gases formed in reaction include CO, CO_2, CH_4, C_2H_6, and C_3H_8; liquid byproducts include diethyl ether, acetaldehyde, butyraldehyde, ethyl acetate, and several unidentified components that were counted as liquid products. The quantities of all products formed in reaction are given in Table S1 of the Supplementary Information.

Table 1. Results of ethanol conversion to higher alcohols in fixed bed reactor

Temp (^oC)	WHSV (h^{-1})	Ethanol Conversion %	Selectivity (%)				Carbon recovery (%)
			n-Butanol	C_6+ Alcohols	Gases	Liquid byproducts	
1 wt% Ni/9 wt% La_2O_3/γ-Al_2O_3							
210	1.4	7	68	11	6	16	99
230	0.8	22	58	21	9	9	97
230	1.4	15	62	17	8	11	98
230	2.1	12	63	14	8	12	97
250	0.8	41	51	23	15	8	97
250	1.4	29	54	21	12	11	98
250	2.1	23	58	10	11	11	91
8 wt% Ni/4.5 wt% La_2O_3/γ-Al_2O_3							
210	0.8	29	59	14	22	9	102
210	1.1	26	57	13	18	10	88
210	1.4	23	58	13	16	13	100
210	1.8	22	56	13	15	11	95
230	1.4	42	46	13	28	10	97

4. Process Concept

The initial results in a continuous fixed bed reactor form the basis for a process to convert ethanol to n-butanol and higher alcohols. The process concept consists of the reactor for ethanol conversion and a separation train to produce pure n-butanol and a mixture of C_6+ alcohols as saleable products. In contrast to some other reports of Guerbet reaction processes (Michaels et al., 2018; Dias et al., 2014; Pereira et al., 2014; Pereira et al., 2015a; Pereira et al., 2015b), in this work minor gas and liquid byproducts are burned as fuel for steam generation to provide energy for the process; capital and operating expenditures to recover them as pure products are not justified because of their low concentration in the product mix.

The ethanol-to-higher alcohols Guerbet reaction process is intended to be located adjacent to an ethanol plant, and thus there are two strategies for configuring the combined facility. The first approach, used in several economic analyses of Guerbet reactions with sugar cane-based ethanol production (Dias et al., 2014; Pereira et al., 2014; Pereira et al., 2015a; Pereira et al., 2015b), is to pass the entire product stream from ethanol fermentation through the Guerbet process, wherein partial conversion to higher alcohols takes place and the unreacted ethanol becomes the primary plant output. The second approach, adopted in this work, is to divert only a portion of the product ethanol to the Guerbet process, and then recycle unreacted ethanol within the Guerbet process to give an overall conversion approaching 100%.

The key reaction parameter for most renewables-based chemical processes is selectivity to desired products. In this ethanol condensation process, both selectivity and ethanol conversion

are important, because reactions are sequential and thus selectivity depends on conversion. Further, because the overall process conversion of ethanol is essentially 100%, the extent of ethanol recycle and thus distillation column size depends on per-pass reactor conversion. To illustrate the dependence of process economics on these parameters, a set of four base cases with different combinations of ethanol conversion and alcohol selectivities is examined. These are designated by the two-digit ethanol conversion percentage and either "L" for low (60% n-butanol, 16% C_6+ alcohols) selectivity or "H" for high (72% n-butanol, 22% C_6+ alcohols) selectivity. The case designated 35L (35% ethanol conversion, low selectivity) represents results obtained in the experimental fixed-bed reactor studies reported in Table 1. The other cases (40L, 35H, 70H) reflect higher ethanol conversion or selectivity, in order to ascertain future potential for n-butanol production via ethanol condensation.

The flow diagram used as the basis for the Aspen Plus V8.4 simulation of the four base cases for the proposed ethanol condensation process is given in Figure 3. Fresh ethanol (Stream F) is combined with recycled ethanol (S6), pressurized to 100 bar, and preheated to the reaction temperature of 230 ^{o}C in heat exchangers H1 and H2. The reactor (FBR) is a fixed-bed shell and tube reactor in which the heat of reaction generated on the tube side, where catalyst is loaded, is removed by generating steam on the shell side at approximately 230 ^{o}C. This steam is used to partially preheat the reactor feed in H1.

The effluent stream (S2) from the fixed-bed reactor is partially flashed from 100 bar to a lower pressure (Valve V1) and fed to Column TC1, where ethanol, water, and light byproducts are taken as the distillate (S3) and n-butanol, mixed C_6+ alcohols, and in some cases water exit as the bottoms stream (S8) of TC1. Further details regarding the ethanol/n-butanol separation carried out in Column TC1 are given below, along with an explanation of the two process alternatives highlighted in Figure 3 for recovering pure n-butanol and mixed C_6+ alcohols. The light byproducts formed in reaction (chosen for simulation as ethyl acetate, diethyl ether, CH_4, CO_2, and H_2, see Table S1 for the complete byproduct slate) are recovered as a mixed distillate stream (S4) in Column TC2 and used as fuel for steam generation. The bottoms stream from Column TC2, consisting of ethanol and water, is separated in Column TC3 into an azeotropic ethanol/water mixture (S6) for recycling and pure water (S7) as a bottoms product.

Several pressures were examined in preliminary simulations of the separation train; an absolute pressure of 5.0 bar was chosen for columns TC1 and TC2, and an absolute pressure of 1.0 bar was chosen for Column TC3 and the n-butanol/C_6+ alcohol separation (Column TC4 or Columns TC4-TC6). These pressures are high enough to allow column condensers to operate with air cooling instead of refrigeration, yet are low enough to avoid excessively high temperatures in column reboilers. Other combinations of pressures could conceivably further improve process efficiency and economics, but no other pressure combinations were evaluated in this work.

The two process alternatives highlighted in the lower right side of Figure 3 represent two process scenarios depending on whether or not Stream S8 from Column TC1 contains water. If Stream S8 is dry, then n-butanol and C_6+ alcohols are separated in Column TC4 into pure (99.87

± 0.04 mol%) n-butanol (S9) and C_6+ alcohols (chosen for simulation as equimolar quantities of 1-hexanol and 2-ethyl-1-butanol, together >99.75 mol% in S10) as shown in the upper block in Figure 3. If Stream S8 contains water, then C_6+ alcohols are recovered as the bottoms stream (>99.75 mol%, S12) of Column TC4, and the distillate (S11) of Column TC4 containing n-butanol and water, which form a heterogeneous azeotrope, is separated using the classic approach of two distillation columns (TC5 and TC6) with a decanter as shown in the lower block in Figure 3. Capital and operating costs associated with this latter approach are significant, as the n-butanol-water separation columns (TC5 and TC6) require high reflux ratios and recycling of intermediate streams to obtain dry (99.87 ± 0.04 mol%) n-butanol.

The composition of the reactor effluent (Stream S2) entering Column TC1 determines whether or not Stream S8 from Column TC1 contains water, and thus which of the two process scenarios above is used. The ethanol/water/n-butanol residue curve map shown in Figure 4 (generated using the S-R Polar equation of state in Aspen Plus V8.4) illustrates the two cases. In this residue curve map, a distillation boundary arises because ethanol and n-butanol both form minimum-boiling azeotropes with water. If C_6+ alcohol products (recovered in Column TC4) and light byproducts (recovered in Column TC2) are momentarily neglected, so that Columns TC2 and TC4 can be neglected and Stream S5 can be considered equivalent to Stream S3 in Figure 3, then the residue curve map in Figure 4 applies directly to Columns TC1 and TC3.

If sufficient ethanol is present in the reactor effluent (S2), generally corresponding to a maximum per-pass ethanol conversion in the FBR of 40% (Cases 35L, 35H, 40L), then all water in Stream S2 (both produced in reaction and present in the reactor feed) can be removed with ethanol into the distillate (S3) of Column TC1. Negligible n-butanol is carried to the distillate (S3), leaving dry n-butanol as the bottoms product of TC1. This separation is represented as the straight line S8-S2-S3 for Case 35L in Figure 4; the distillate (S3) composition lies close to the distillation boundary and contains less than 0.001 mole fraction n-butanol, while the bottoms (S8) composition approaches pure n-butanol. Separation of the distillate mixture (S3 equivalent to S5 without light byproducts present) in the subsequent Column TC3, represented by the line S7-S3-S6 for Case 35L in Figure 4, produces the ethanol-water azeotrope as distillate (S6) and water containing trace n-butanol as the bottoms product (S7). This separation in Column TC3 crosses the distillation boundary on the residue curve map. While crossing the distillation boundary is not usually possible, such crossings are possible in cases where the boundary has significant curvature (Fidkowski et al., 1993). To ensure that crossing the distillation boundary in the Aspen Plus V8.4 simulation of this system was not an artifact of the S-R Polar properties package, the ethanol/n-butanol/water residue curve map was also generated and the separations in Columns TC1 and TC3 were also simulated using the Non-Random Two Liquid (NRTL) properties package. The same results were obtained using the NRTL properties package as with the S-R Polar equation of state; the use of very different thermodynamic properties packages to obtain the same result provides validation of the crossing of the distillation boundary and the separations in Columns TC1 and TC3.

As per-pass ethanol conversion in the FBR increase above 40% (Case 70H), the reactor effluent (S2) contains less ethanol and more water and n-butanol, thus shifting point S2 in Figure 4 away from the ethanol vertex of the residue curve map (to 41 mol% H_2O, 32 mol% ethanol, and 27 mol% n-butanol for Case 70H). Attempting to recover pure n-butanol from Column TC1 as this shift in S2 occurs would result in ~8 mol% n-butanol in the distillate stream (S3) from Column TC1, as Stream S3 is limited in composition by the distillation boundary. This n-butanol in the distillate Stream S3 from Column TC1 would be lost from the process, or would have to be recovered via additional separation. Thus, for high ethanol conversion in the FBR, a different separation in Column TC1 must be carried out. This separation is shown as the line S3-S2-S8 for Case 70H in Figure 4, where an ethanol-water mixture is taken as the distillate stream (S3) and a binary mixture of n-butanol and water is taken as the bottoms product (S8). The binary n-butanol/water mixture is then separated into pure n-butanol and pure water with the two column and decanter system shown in the lower box in Figure 3.

In the actual process simulation of Column TC1 with the complete reactor effluent (Stream S2), the light byproducts formed in reaction rapidly move upward in the vapor phase of Column TC1 and have little influence on the ethanol/n-butanol separation. The C_6+ alcohols in Stream S2, which have low miscibility with water, move rapidly downward in the liquid phase of Column TC1 and actually aid in facilitating the separation of water from n-butanol in Column TC1 as described above.

It is noted here that there are other scenarios possible for recovery of n-butanol from mixed alcohol streams. Patrascu (Patraşcu et al., 2017) propose a double wall distillation column integrated with other columns to recovery dry butanol from ABE fermentation broth. Pervaporation has also been examined as another route to recovery of butanol from fermentation (Kießlich et al., 2017). Michaels et al. (Michaels et al., 2018) describe the use of benzene to break the butanol-water azeotrope in an ethanol condensation reaction process.

Energy for distillation reboilers and heating process streams is provided by high pressure steam at 257 ^{o}C and 45 bar produced in a steam generator fueled by natural gas and by the light byproducts from the Guerbet reaction. Because the plant is proposed to be located adjacent to an ethanol facility and not necessarily close to an external cooling water source, for the base case analysis all energy removed from the process (reactor, coolers, and column condensers), if not used elsewhere for heating, is ultimately rejected to air via air-cooled heat exchangers. The use of external water cooling is examined as an alternate process configuration.

5. Techno-Economic Analysis

5.1 Definition of design parameters

Capital and operating costs for ethanol conversion to higher alcohols have been evaluated from Aspen Plus V8.4 simulations with the SR-Polar equation of state as the properties package (Jordison et al., 2015). The four base case scenarios and several variations of the base process concept shown in Figure 3 have been examined. The outcome of the analysis determines the

required selling price of n-butanol for these different cases as a function of return on investment (ROI). As in any economic analysis, assumptions must be made, and values of parameters defined, in order to properly carry out the calculations. General design parameters used in the techno-economic analysis are summarized in Table 2 below; additional parameters defining unit operations for specific cases are given in Table S2 and Table S3 of the Supplementary Information.

Table 2. Parameters for techno-economic analysis

Parameter	Value
Location	Midwest U.S.
Plant Capacity (10^6 kg n-Butanol/yr)	75 (25 million gallons)
Plant Lifetime	10 years
Ethanol feed cost	$0.53/kg ($1.65/gallon)
C_6+ alcohol selling price ($/kg)	0.75 x n-butanol selling price
UTILITIES	
Natural gas cost	$3.21/$10^6$ kJ ($3.39/$10^6$ Btu)
Electricity cost	$18.6/$10^6$ kJ ($0.067/kWh)
Cooling water cost	$14.80/$10^3$ m^3
GENERAL DESIGN PARAMETERS	
REACTOR	
Tube size	2.5 cm 20 BWG, 316 SS
Tube spacing	3.2 cm triangular centers
Catalyst particle diameter	2.0 mm
Catalyst cost (8% Ni/8% La_2O_3/γ-Al_2O_3)	$100/kg
DISTILLATION COLUMNS	
Tray type	Sieve
Tray efficiency	60%
Tray spacing	0.61 m
Approach to flooding	80%
AIR-COOLED HEAT EXCHANGERS AND CONDENSERS	
Configuration	Forced-air finned tube
Heat transfer coefficient (bare tube area basis)	770 W/m^2/K
Fin area / bare tube area ratio	17
REBOILERS	
Configuration	Shell and tube, single pass
Energy source	Steam (45 bar, 257 ^oC)
Heat transfer coefficient	850 W/m^2/K
WATER- or GLYCOL-COOLED HEAT EXCHANGERS	
Configuration	Shell and tube, single pass
Heat transfer coefficient	680 W/m^2/K

Location and scale for an initial butanol-from-ethanol facility fit with existing U.S. ethanol production facilities. The price of ethanol ($1.65/gallon, or $0.53/kg) is taken as the average wholesale price over a one year period of 2016-2017 (Ethanol Historical Prices, 2017); across-the-fence prices would be expected to be lower. Utility prices are taken as conservative values for the Midwestern U.S. (Electric Power Monthly, 2017; U.S. Natural Gas Prices, 2017); a sensitivity analysis of process economics vs. ethanol price and utility prices is presented later in this document. Reactor and distillation column specifications are taken from standard references (Couper et al., 2005; Purohit, 1983) and are typical for initial process equipment design. Catalyst cost is conservatively estimated, as nickel and lanthanum oxide are both inexpensive materials. Air-cooled heat exchanger properties are taken from a handbook on air-cooled exchanger design (Process Engineering Guide: Air Cooled Heat Exchanger Design, n.d.); heat transfer coefficients for shell and tube heat exchangers were taken as conservative (low) values within the range of typical coefficients for each type of heat exchanger (Kern, 1983).

In the Aspen Plus simulations, the fixed bed reactor is simulated using the RStoic module with the required catalyst volume calculated from simple second-order kinetics of ethanol conversion with a fixed value of the rate constant ($k = 5.7 \times 10^{-5}$ m^6/kmol EtOH/kg cat/h). Fixing the catalyst activity for all four cases allows comparison of the effect of selectivity on economics (cases 35L vs. 35H) and the comparison of designated per-pass conversion on economics (35L vs. 40L; 35H vs. 70H). In addition, in our prior work (Jordison et al., 2016) we reported that small quantities of water present in the ethanol feed have little effect on conversion rate – for that reason, we neglect that up to 2.7 wt% water, which comes from ethanol recycle (Stream S6) as the azeotropic composition with water, may be present in the ethanol feed stream (S1) to the reactor.

Distillation columns are simulated using the rigorous column module RadFrac. Number of stages and reflux ratios are adjusted to achieve desired product purities from each column. Cases 35L, 35H, and 40L use the single-column block in the lower part of Figure 3 to separate n-butanol from C_6+ alcohols; Case 70H uses the three column plus decanter block in Figure 3 to produce the C_6+ alcohol product and dry n-butanol. The specifications of each piece of equipment from the Aspen Plus V8.4 simulation are entered into an in-house Excel spreadsheet that includes standard formulas for calculating the purchase cost of individual pieces of equipment (Buthod, 2001; Couper et al., 2005; D. Q. Kern, 1983; McKetta, 1994; Primo, 2012; Process Engineering Guide: Air Cooled Heat Exchanger Design, n.d.; Purohit, 1983); these cost formulas and the reactor and distillation column specifications for each case are given in Table S2 of the Supplementary Information. Specifications for the heat exchangers in Case 35L, including column reboilers and condensers, are given in Table S3 in Supplementary Information.

To determine total capital costs of the process, individual equipment purchase costs are summed and multiplied by standard multipliers for installation, facilities, engineering, working capital, etc. to arrive at the total capital costs for the process, which is then normalized with the CPI index to 2016 $US (Economic Indicators, 2017). Operating costs are similarly determined by

entering raw material and utility requirements for each unit operation and using standard multipliers as required for labor, site maintenance, marketing, taxes, etc. (Peters et al., 2003). The multipliers used in calculation of various contributions to the overall process economic analysis are given in Table 3, where total capital costs and operating costs for each of the four cases are presented.

Depreciation of plant capital costs (10 years, straight line) is combined with operating costs and feed stock costs to determine a total cost of production of n-butanol. This value is subtracted from product sale income to give annual net revenue, which is readily converted to an estimated annual return on investment.

5.2 Results of Techno-Economic Analysis

5.2.1 Base cases

The compositions and flow rates of each of the streams in Figure 3 for Case 35L are given in Table S4 in the Supplementary Information. The energy demands for each column reboiler and condenser, and for each heat exchanger for Case 35L are shown in Figure 3. A summary of total plant capital costs and operating costs for the four base cases is given in Table 3 below. A graph of required n-butanol selling price versus desired ROI for the cases is presented in Figure 5.

Table 3. Economic analysis of base cases (Basis: 25 million gallons (75 million kg) n-butanol/yr)

Case (Ethanol conversion, Selectivity)		35L	40L	35H	70H
Ethanol conversion (%)		35	40	35	70
n-Butanol selectivity (%)		60	60	72	72
C_6+ alcohol selectivity (%)		16	16	22	22
Parameter	Reference				
CAPITAL COSTS (10^6 $)					
Equipment Purchase Cost (PC)	Calculated	9.14	8.33	7.64	9.61
Instrumentation, controls	1.21 PC	11.02	10.05	9.21	11.59
Facility	0.75 PC	6.77	6.18	5.66	7.12
Contractor, engineering	0.82 PC	7.47	6.81	6.24	7.86
Contingency	5% CAPEX	1.88	1.72	1.57	1.98
Working Capital	5% CAPEX	1.81	1.65	1.52	1.91
TOTAL CAPITAL COSTS (CAPEX)		38.09	34.75	31.84	40.07
OPERATING COSTS (10^6 $/yr)					
Raw Materials	Calculated	88.05	89.26	73.83	75.75
Utilities	Calculated	5.10	3.81	6.13	2.58
Labor and maintenance	6% OPEX	8.18	7.89	6.93	7.46
Laboratory / Analytical	1% OPEX	1.30	1.26	1.10	1.16
Royalties / Licensing Fees	2% OPEX	2.68	2.64	2.28	2.30
Fixed Costs[a]	16% CAPEX	6.21	5.66	5.19	6.53
Overhead	6% OPEX	8.04	7.92	6.84	6.90

General Expenses[b]	11% OPEX	14.35	13.96	12.17	12.75
TOTAL OPERATING COSTS (OPEX)	(10^6 $/yr)	133.90	132.42	114.47	115.43

[a]Fixed costs include capital depreciation, taxes, and insurance

[b]General Expenses include administration, distribution and selling costs, R&D, and financing costs

Figure 5 shows that producing n-butanol via catalytic ethanol Guerbet condensation has significant potential for chemical applications of n-butanol, especially if higher selectivity to the desired alcohol products can be achieved. At present, n-butanol market prices range from $1.30/kg to $2.00/kg (Chem-Net Facts: n-Butanol, 2013; Mariano et al., 2013) depending on geographic location, so the required selling price reflected in Figure 5 falls in the range of those values under most conditions. It should be noted that n-butanol potential as a fuel component or oxygenate in gasoline in the U.S. is not economical in the present scenario, as n-butanol does not compete with current ethanol ($0.50-0.60/kg) or gasoline ($0.80-1.00/kg) prices.

The economic analysis shows that increasing the per-pass ethanol conversion from 35% to 40% at low selectivity values reduces required selling price of n-butanol, because the ethanol recycle stream and thus the quantity of ethanol fed to the reactor are smaller at higher conversion. Increasing ethanol conversion also reduces utility costs, as the contribution of the light byproducts formed to overall energy requirements for the process increases from 50% for Case 35L to 60% for case 40L, reducing utility costs by $1.3 million annually.

Required n-butanol selling price increases when per-pass conversion is increased from 35% to 70% at high selectivity, because 1) a much larger reactor is required to achieve 70% conversion, and 2) the smaller quantity of ethanol in the reactor effluent (S2) at 70% conversion requires that the n-butanol/water azeotrope be broken with the traditional two column/decanter approach shown in the lower block of Figure 3. Thus, for this process, the preferred design is to run the reactor at a per-pass conversion of 35-40% to lower capital costs and avoid having to separate the n-butanol/water azeotrope using multiple columns. Of course, if a more active catalyst can be developed, then the higher per pass conversion through the reactor may become preferred.

5.2.2 Sensitivity Analysis of Key Cost Drivers

An analysis of n-butanol required selling price dependence on ethanol feed cost, equipment purchase cost, and utility costs has been carried out for Case 35L. For each of these parameters, the effect of increasing the base case value by 10%, 20%, and 30% on n-butanol required selling price has been evaluated. All other cost calculations in each case are scaled according to guidelines given in Table 3. Results for the complete range of ROI are given in Figures S1 – S3 in the Supplementary Information. For 25% ROI, increasing equipment purchase cost by 30% (from $9.14 million to $11.88 million) increases the required n-butanol selling price by $0.09/kg (Figure S1). For the same ROI, increasing ethanol feed cost by 30% (from $1.65/gallon to $2.15/gallon) increases the required n-butanol selling price by $0.36/kg (Figure S2). Finally, at the same ROI, increasing total utility (natural gas + electricity) costs by 30% (from $5.10 million

to $6.33 million) increases the required n-butanol selling price by $0.02/kg (Figure S3). Clearly, the process economics for n-butanol production from ethanol are most heavily affected by ethanol feed cost.

5.2.3 Alternate Process Configurations

In addition to the four base cases examined, several alternate design scenarios have been simulated in Aspen Plus V8.4, and the techno-economic analysis has been carried out for each scenario. The results of these analyses are described in the following paragraphs.

Two-fold process scale-up: Case 35L was simulated and analyzed for n-butanol production of 150 million kg (50 million gallons) per year, twice the size of the base case capacity. Capital cost increased from $38.1 million to $71.1 million; operating costs related to raw materials and utilities essentially double for the larger scale. The overall reduction in required n-butanol selling price in scaling up to 150 million kg/yr from 75 million kg n-butanol annually is $0.03/kg n-butanol at 25% ROI.

Heat integration – The process configuration in Figure 3 with the specified process pressures offers the opportunity for heat integrating the condensers of columns TC1 (121-122 ^{o}C) and TC4 (118 ^{o}C) with the reboiler of TC3 (99 ^{o}C). The heat-integrated process does not require a dedicated heat exchanger or utilities for the condensers of TC1 and TC4, but instead, direct heat exchange can take place between the distillate vapor streams of TC1 and TC4 and the reboiler liquid of TC3. Heat integration reduces the overall utility costs for the process from $5.1 million to $3.2 million annually. A smaller steam generator is also required for the heat integrated case. Unfortunately, modestly larger heat exchangers are required for the heat integrated process, because thermal driving forces are smaller. Because of this, total capital costs for the heat integrated process are $38.5 million vs. $38.1 million for base case 35L. But overall, the required selling price of n-butanol for an ROI of 25% is approximately $0.03/kg lower for the heat integrated case than for the base case 35L.

Drying of ethanol/water recycle stream: In the base-case process, unreacted ethanol is recycled as its azeotropic composition with water (Stream S6 in Figure 3); it is assumed, based on our prior studies (Jordison et al., 2016), that the recycled water has a negligible effect on ethanol conversion and selectivity to higher alcohols. Nevertheless, the cost of removing water from the ethanol recycle stream (S6) via a conventional two-unit pressure swing molecular sieve unit was estimated for Case 35L. The molecular sieve unit is assumed to adsorb at 1.7 bar absolute and regenerate at 0.14 bar absolute, with 10% of the dry product ethanol stream directed to regeneration of the saturated bed with an 8 h cycle time. The purchase cost of the molecular sieve unit is $2.48 million (Bastidas et al., 2012; Dale and Tyner, 2006), which increases the total process CAPEX from $38.1 million to $47.7 million. Utility costs are essentially unchanged with addition of the molecular sieve unit, as the absence of water in S6 reduces the reboiler loads in

separation to offset the increased reboiler duty in TC3 from the regenerating ethanol stream. The increased capital and operating costs associated with the molecular sieve unit together increase the required n-butanol selling price at 25% ROI by $0.07/kg n-butanol.

It is worth noting that removing water from the recycle stream (S6) makes the process equivalent to a process with once-through ethanol flow of a rate equal to Stream S1 and the same conversion and selectivity. The increase in cost noted above results from drying unreacted ethanol via molecular sieve before sending it to market. Similarly, the base cases are also equivalent to a process with once-through ethanol feed at a rate equal to S1 where only part of the feed ethanol and the exiting wet ethanol are dried by molecular sieves.

Method of Heat Removal: The four cases reported in Table 3 use direct air cooling in forced air convection heat exchangers to remove process heat from distillation column condensers and the intercooler between TC1 and TC2. These exchangers are sized according to heat load and approach ΔT, and the electrical power requirements for the fans are included in utility costs for the processes (Process Engineering Guide: Air Cooled Heat Exchanger Design, n.d.). The process design for Case 40L has also been carried out with two alternative heat exchange systems: 1) the use of cooling water from an external source or cooling ponds on-site in direct exchange with process streams; and 2) a closed-loop glycol cooling system in which process energy is removed via glycol cooling and the glycol is cooled in a secondary air-cooled heat exchanger. For cooling with an external water source, the incoming water is assumed to be at 25 ^{o}C and a maximum cooling water ΔT of 10 ^{o}C. With these design parameters, cooling water demand for the process is 5.3 x 10^3 m^3/h. For the closed-loop coolant, two heat exchangers are required for each location, leading to an increase in capital and operating cost. This increase in capital cost results from the large heat exchanger areas required, as the overall temperature driving force for heat removal to air must be divided between two heat exchangers. This renders the cost of a facility with closed loop cooling substantially more expensive, as seen in Table 4. The higher costs render the closed loop cooling unattractive; the only likely advantage of such a system would be improved control of condenser heat duty and temperature. In contrast, external water cooling, if such a source is available, is slightly less expensive than air cooling, and has advantages of reduced noise and possible mechanical failures related to air-cooled heat exchange. Returning external water to a river or lake has possible environmental consequences regarding thermal pollution, so cooling ponds are preferable alternatives if makeup water and sufficient space are available.

Table 4. Capital and operating costs for different heat removal options for Case 40L

Parameter	Air cooling	Glycol closed loop / Air	External water

TOTAL Capital Costs (CAPEX) (10^6)	34.7	66.5	32.5
Utilities (10^6/yr)	3.81	4.17	4.30
TOTAL Production Costs (10^6/yr)	132.4	144.8	132.3
Required n-butanol selling price at 25% ROI ($/kg)	1.56	1.78	1.55

Alternate Location of Ethanol Feed: As stated earlier, for Case 70H (70% ethanol conversion) there is insufficient ethanol present in the reactor effluent to remove all water produced in reaction to the distillate of Column TC1 without taking substantial n-butanol into the distillate as well. To further examine the possibility of improving the economics of Case 70H, an alternate scenario was examined in which fresh ethanol to the process is fed into Column TC1 instead of into the FBR. Simulation of this configuration shows that dry n-butanol can be produced as a bottoms of Column TC1 with little n-butanol in the distillate (similar to Column TC1 represented as the line S8-S2-S3 for Case 35L in Figure 4), thus eliminating the need for the two column/decanter system to separate the n-butanol/water azeotrope. However, the economic analysis shows that feeding fresh ethanol to Column TC1 leads to substantial increases in capital and utility costs of Columns TC1, TC2, and TC3 that more than offset the capital and operating cost savings from eliminating the butanol/water separation columns. At 25% ROI, the required n-butanol selling price with ethanol fed to Column TC1 is $1.45/kg, as opposed to $1.35/kg for the base case 70H where fresh ethanol is fed to the FBR. Thus, the alternate ethanol feed location is impractical, despite the fact that it eliminates separating the n-butanol/water azeotrope using two columns and the decanter.

6. Conclusions

The continuous condensed-phase reaction of ethanol to n-butanol and C_6+ alcohols has been demonstrated in a laboratory fixed bed reactor. Based on experimental results and analysis of phase equilibria for this system, a process concept has been developed that converts all ethanol and produces pure n-butanol and a mixed higher (C_6+) alcohols stream as products, while minor byproducts formed are burned to provide process energy. The process has been simulated in Aspen Plus V8.4 for several combinations of per-pass ethanol conversion and selectivity to product alcohols, and an economic analysis of each combination has been carried out. For n-butanol selectivities achieved in laboratory studies, the required selling price is $1.55-$1.60/kg, close to current n-butanol selling prices for chemical applications. If selectivity to higher alcohols can be improved, then the production of n-butanol and C_6+ alcohols from ethanol for use as industrial chemicals becomes attractive.

Acknowledgments

This work was supported by the U.S. Department of Energy (Award DE-FG36-04GO14216) through a subcontract with the National Corn Growers Association, and by the Michigan State University AgBioResearch Center. The authors thank Dr. Chris Saffron for helpful discussions with the economic analysis.

References

Algayyim, S.J.M., Wandel, A.P., Yusaf, T., Hamawand, I., 2018. Production and application of ABE as a biofuel. Renew. Sustain. Energy Rev. 82, 1195–1214. https://doi.org/10.1016/j.rser.2017.09.082

Bastidas, P., Parra, J., Gil, I., Rodríguez, G., 2012. Alcohol distillation plant simulation: Thermal and hydraulic studies. Procedia Eng. 42, 80–89. https://doi.org/10.1016/j.proeng.2012.07.397

Brito, M., Martins, F., 2017. Life cycle assessment of butanol production. Fuel 208, 476–482. https://doi.org/10.1016/j.fuel.2017.07.050

Buthod, P., 2001. Pressure Vessel Handbook, 12th ed. Pressure Vessel Publishing Inc, Tulsa, Oklahoma.

Chem-Net Facts, Chemical Market Insight and Foresight - on a Single Page: n-Butanol, 2013. , Tecnon OrbiChem. URL http://www.orbichem.com/userfiles/CNF Samples/act_13_11.pdf

Chieregato, A., Ochoa, J.V., Bandinelli, C., Fornasari, G., Cavani, F., Mella, M., 2015. On the chemistry of ethanol on basic oxides: Revising mechanisms and intermediates in the Lebedev and Guerbet reactions. ChemSusChem 8, 377–388. https://doi.org/10.1002/cssc.201402632

Couper, J.R., Penny, W.R., Fair, J.R., 2005. Chemical Process Equipment: Selection and Design, 2nd ed, Gulf Professional Publishing, Oxford, England.

Dale, R.T., Tyner, W.E., 2006. Economic and technical analysis of ethanol dry milling: model description. http://purl.umn.edu/28674

De Gennes, P.-G., 1909. Condensation de l'alcool isopropylique avec son dérivé sodé; formation du méthylisobutylcarbinol et du diméthyl-2.4-heptanol-6. Comptes rendus l'Académie des Sci. 149, 129–132.

Dias, M., Pereira, L.G., Junqueira, T.L., Pavanello, L.G., Chagas, M.F., Cavalett, O., Maciel Filho, R., Bonomi, A., 2014. Butanol production in a sugarcane biorefinery using ethanol as feedstock. Part I: Integration to a first generation sugarcane distillery. Chem. Eng. Res. Des. 92, 1441–1451. https://doi.org/10.1016/j.cherd.2014.04.030

Economic Indicators, 2017. Chem. Eng. 124, 104. https://doi.org/10.1016/S1470-2045(17)30641-1

Electric Power Monthly, 2017. Energy Information Administration URL http://www.eia.gov/dnav/ng/ng_pri_sum_dcu_nus_a.htm

Ethanol Historical Prices [WWW Document], 2017. Bus. Insid. URL https://markets.businessinsider.com/commodities/historical-prices/ethanol-price/25.4.2016_25.4.2017

Fidkowski, Z.T., Doherty, M.F., Malone, M.F., 1993. Feasibility of separations for distillation of nonideal ternary mixtures. AIChE J. 39, 1303–1321. https://doi.org/10.1002/aic.690390806

Fraas, A.P., 1989. Heat Exchanger Design. Wiley-Interscience Publication, New York.

Gabriëls, D., Hernández, W.Y., Sels, B., Van Der Voort, P., Verberckmoes, A., 2015. Review of catalytic systems and thermodynamics for the Guerbet condensation reaction and challenges for biomass valorization. Catal. Sci. Technol. 5, 3876–3902. https://doi.org/10.1039/C5CY00359H

Ghaziaskar, H.S., Xu, C. (Charles), 2013. One-step continuous process for the production of 1-butanol

and 1-hexanol by catalytic conversion of bio-ethanol at its sub-/supercritical state. RSC Adv. 3, 4271. https://doi.org/10.1039/c3ra00134b

Green, E.M., 2011. Fermentative production of butanol-the industrial perspective. Curr. Opin. Biotechnol. 22, 337–343. https://doi.org/10.1016/j.copbio.2011.02.004

Hernández, W.Y., De Vlieger, K., Van Der Voort, P., Verberckmoes, A., 2016. Ni−Cu Hydrotalcite-Derived Mixed Oxides as Highly Selective and Stable Catalysts for the Synthesis of β-Branched Bioalcohols by the Guerbet Reaction. ChemSusChem 9, 3196–3205. https://doi.org/10.1002/cssc.201601042

Ho, C.R., Shylesh, S., Bell, A.T., 2016. Mechanism and Kinetics of Ethanol Coupling to Butanol over Hydroxyapatite. ACS Catal. 6, 939–948. https://doi.org/10.1021/acscatal.5b02672

Jordison, T.L., Lira, C.T., Miller, D.J., 2015. Condensed-Phase Ethanol Conversion to Higher Alcohols. Ind. Eng. Chem. Res. 54, 10991–11000. https://doi.org/10.1021/acs.iecr.5b02409

Jordison, T.L., Peereboom, L., Miller, D.J., 2016. Impact of Water on Condensed Phase Ethanol Guerbet Reactions. Ind. Eng. Chem. Res. 55, 6579–6585. https://doi.org/10.1021/acs.iecr.6b00700

Kern, D., 1983. Process Heat Transfer. McGraw Hill International Book Company, Tokyo, Japan.

Khamaiseh, E.I., Abdul Hamid, A., Abdeshahian, P., Wan Yusoff, W.M., Kalil, M.S., 2014. Enhanced butanol production by Clostridium acetobutylicum NCIMB 13357 grown on date fruit as carbon source in P2 medium. Sci. World J. 2014. https://doi.org/10.1155/2014/395754

Kießlich, S., Sarchami, T., Munch, G., Gao, K., Rehmann, L., Kujawski, W., Johnson, E., 2017. Pervaporative butanol removal from PBE fermentation broths for the bioconversion of glycerol by Clostridium pasteurianum. J. Memb. Sci. 535, 79–88. https://doi.org/10.1016/j.memsci.2017.04.012

Kozlowski, J.T., Davis, R.J., 2013. Heterogeneous catalysts for the Guerbet coupling of alcohols. ACS Catal. 3, 1588–1600. https://doi.org/10.1021/cs400292f

Levasseur, A., Bahn, O., Beloin-Saint-Pierre, D., Marinova, M., Vaillancourt, K., 2017. Assessing butanol from integrated forest biorefinery: A combined techno-economic and life cycle approach. Appl. Energy 198, 440–452. https://doi.org/10.1016/j.apenergy.2017.04.040

Lodi, G., De Guido, G., Pellegrini, L.A., 2018. Simulation and energy analysis of the ABE fermentation integrated with gas stripping. Biomass and Bioenergy 116, 227–235. https://doi.org/10.1016/j.biombioe.2018.06.012

Marcu, I.C., Tanchoux, N., Fajula, F., Tichit, D., 2013. Catalytic conversion of ethanol into butanol over M-Mg-Al mixed oxide catalysts (M = Pd, Ag, Mn, Fe, Cu, Sm, Yb) obtained from LDH precursors. Catal. Letters 143, 23–30. https://doi.org/10.1007/s10562-012-0935-9

Mariano, A.P., Dias, M.O.S., Junqueira, T.L., Cunha, M.P., Bonomi, A., Filho, R.M., 2013. Butanol production in a first-generation Brazilian sugarcane biorefinery: Technical aspects and economics of greenfield projects. Bioresour. Technol. 135, 316–323. https://doi.org/10.1016/j.biortech.2012.09.109

McKetta, J.J., 1994. Encyclopedia of Chemical Processing and Design: Volume 50. Marcel Dekker Inc, New York.

Michaels, W., Zhang, H., Luyben, W.L., Baltrusaitis, J., 2018. Design of a separation section in an ethanol-

to-butanol process. Biomass and Bioenergy 109, 231–238. https://doi.org/10.1016/j.biombioe.2017.12.031

Nagy, Z.K., 2007. Model based control of a yeast fermentation bioreactor using optimally designed artificial neural networks. Chem. Eng. J. 127, 95–109. https://doi.org/10.1016/j.cej.2006.10.015

Ndaba, B., Chiyanzu, I., Marx, S., 2015. n-Butanol derived from biochemical and chemical routes: A review. Biotechnol. Reports 8, 1–9. https://doi.org/10.1016/j.btre.2015.08.001

Ndou, A.S., Plint, N., Coville, N.J., 2003. Dimerisation of ethanol to butanol over solid-base catalysts. Appl. Catal. A Gen. 251, 337–345. https://doi.org/10.1016/S0926-860X(03)00363-6

Nezam, I., Peereboom, L., Miller, D.J., 2017. Enhanced Acrylate Production from 2-Acetoxypropanoic Acid Esters. Org. Process Res. Dev. 21, 715–719. https://doi.org/10.1021/acs.oprd.7b00047

Ogo, S., Onda, A., Yanagisawa, K., 2011. Selective synthesis of 1-butanol from ethanol over strontium phosphate hydroxyapatite catalysts. Appl. Catal. A Gen. 402, 188–195. https://doi.org/10.1016/j.apcata.2011.06.006

Olson, E.S., Sharma, R.K., Aulich, T.R., 2004. Higher-Alcohols Biorefinery. Appl. Biochem. Biotechnol. 115, 913–932. https://doi.org/10.1385/ABAB:115:1-3:0913

Onyestyák, G., 2018. Carbon supported alkaline catalysts for Guerbet coupling of bioethanol. Period. Polytech. Chem. Eng. 62, 91–96. https://doi.org/10.3311/PPch.10390

Onyestyák, G., Novodárszki, G., Wellisch, Á.F., Valyon, J., Thakur, A.J., Deka, D., 2017. Guerbet self-coupling for ethanol valorization over activated carbon supported catalysts. React. Kinet. Mech. Catal. 121, 31–41. https://doi.org/10.1007/s11144-016-1125-3

Patakova, P., Linhova, M., Rychtera, M., Paulova, L., Melzoch, K., 2013. Novel and neglected issues of acetone-butanol-ethanol (ABE) fermentation by clostridia: Clostridium metabolic diversity, tools for process mapping and continuous fermentation systems. Biotechnol. Adv. 31, 58–67. https://doi.org/10.1016/j.biotechadv.2012.01.010

Patel, A.D., Telalović, S., Bitter, J.H., Worrell, E., Patel, M.K., 2015. Analysis of sustainability metrics and application to the catalytic production of higher alcohols from ethanol. Catal. Today 239, 56–79. https://doi.org/10.1016/j.cattod.2014.03.070

Patraşcu, I., Bîldea, C.S., Kiss, A.A., 2017. Eco-efficient butanol separation in the ABE fermentation process. Sep. Purif. Technol. 177, 49–61. https://doi.org/10.1016/j.seppur.2016.12.008

Pereira, L.G., Chagas, M.F., Dias, M.O.S., Cavalett, O., Bonomi, A., 2015. Life cycle assessment of butanol production in sugarcane biorefineries in Brazil. J. Clean. Prod. 96, 557–568. https://doi.org/10.1016/j.jclepro.2014.01.059

Pereira, L.G., Dias, M.O.S., Junqueira, T.L., Pavanello, L.G., Chagas, M.F., Cavalett, O., Maciel Filho, R., Bonomi, A., 2014. Butanol production in a sugarcane biorefinery using ethanol as feedstock. Part II: Integration to a second generation sugarcane distillery. Chem. Eng. Res. Des. 92, 1452–1462. https://doi.org/10.1016/j.cherd.2014.04.032

Pereira, L.G., Dias, M.O.S., Mariano, A.P., Maciel Filho, R., Bonomi, A., 2015. Economic and environmental assessment of n-butanol production in an integrated first and second generation sugarcane biorefinery: Fermentative versus catalytic routes. Appl. Energy 160, 120–131.

https://doi.org/10.1016/j.apenergy.2015.09.063

Peters, M.S., Timmerhaus, K.D., West, R.E., 2003. Plant Design and Economics for Chemical Engineers, 5th ed, McGraw Hill International Edition, New York.

Pfromm, P.H., Amanor-Boadu, V., Nelson, R., Vadlani, P., Madl, R., 2010. Bio-butanol vs. bio-ethanol: a technical and economic assessment for corn and switchgrass fermented by yeast or Clostridium acetobutylicum. Biomass Bioenergy 34, 515–524. https://doi.org/10.1016/j.biombioe.2009.12.017

Primo, J., 2012. Shell and Tube Heat Exchangers Basic Calculations, PDH Online Course M371. Fairfax, VA.

Process Engineering Guide: Air Cooled Heat Exchanger Design [WWW Document], n.d. . GBH Enterprises Ltd. URL www.academia.edu/3641527/Air_Cooled_Heat_Exchanger_Design (accessed 1.3.18).

Purohit, G.P., 1983. Estimating Costs of Shell and Tube Heat Exchangers. Chem. Eng. 90 (17), 57–67.

Quiroz-Ramírez, J.J., Sánchez-Ramírez, E., Hernández-Castro, S., Segovia-Hernández, J.G., Ponce-Ortega, J.M., 2017. Optimal Planning of Feedstock for Butanol Production Considering Economic and Environmental Aspects. ACS Sustain. Chem. Eng. 5, 4018–4030. https://doi.org/10.1021/acssuschemeng.7b00015

Riittonen, T., Eränen, K., Mäki-Arvela, P., Shchukarev, A., Rautio, A.-R., Kordas, K., Kumar, N., Salmi, T., Mikkola, J.P., 2015. Continuous liquid-phase valorization of bio-ethanol towards bio-butanol over metal modified alumina. Renew. Energy 74, 369–378. https://doi.org/10.1016/j.renene.2014.08.052

Riittonen, T., Toukoniitty, E., Madnani, D.K., Leino, A.-R., Kordas, K., Szabo, M., Sapi, A., Arve, K., Wärnå, J., Mikkola, J.P., 2012. One-Pot Liquid-Phase Catalytic Conversion of Ethanol to 1-Butanol over Aluminium Oxide—The Effect of the Active Metal on the Selectivity. Catalysts 2, 68–84. https://doi.org/10.3390/catal2010068

Sánchez, Ó.J., Cardona, C.A., 2008. Trends in biotechnological production of fuel ethanol from different feedstocks. Bioresour. Technol. 99, 5270–5295. https://doi.org/10.1016/j.biortech.2007.11.013

Scalbert, J., Thibault-Starzyk, F., Jacquot, R., Morvan, D., Meunier, F., 2014. Ethanol condensation to butanol at high temperatures over a basic heterogeneous catalyst: How relevant is acetaldehyde self-aldolization? J. Catal. 311, 28–32. https://doi.org/10.1016/j.jcat.2013.11.004

Silvester, L., Lamonier, J.F., Lamonier, C., Capron, M., Vannier, R.N., Mamede, A.S., Dumeignil, F., 2017. Guerbet Reaction over Strontium-Substituted Hydroxyapatite Catalysts Prepared at Various (Ca+Sr)/P Ratios. ChemCatChem 9, 2250–2261. https://doi.org/10.1002/cctc.201601480

Staggs, K.W., Nielsen, D.R., 2015. Improving n-butanol production in batch and semi-continuous processes through integrated product recovery. Process Biochem. 50, 1487–1498. https://doi.org/10.1016/j.procbio.2015.06.009

Tao, L., He, X., Tan, E.C.D., Zhang, M., Aden, A., 2014. Comparative techno-economic analysis and reviews of n-butanol production from corn grain and corn stover. Biofuels, Bioprod. Biorefining 8, 342–361. https://doi.org/10.1002/bbb.1462

Tsuchida, T., Kubo, J., Yoshioka, T., Sakuma, S., Takeguchi, T., Ueda, W., 2008. Reaction of ethanol over hydroxyapatite affected by Ca/P ratio of catalyst. J. Catal. 259, 183–189.

https://doi.org/10.1016/j.jcat.2008.08.005

Tsuchida, T., Sakuma, S., Takeguchi, T., Ueda, W., 2006. Direct Synthesis of n -Butanol from Ethanol over Nonstoichiometric Hydroxyapatite. Ind. Eng. Chem. Res. 45, 8634–8642. https://doi.org/10.1021/ie0606082

U.S. Natural Gas Prices, 2017. Energy Information Administration. URL http://www.eia.gov/dnav/ng/ng_pri_sum_dcu_nus_a.htm

Uyttebroek, M., Van Hecke, W., Vanbroekhoven, K., 2015. Sustainability metrics of 1-butanol. Catal. Today 239, 7–10. https://doi.org/10.1016/j.cattod.2013.10.094

Väisänen, S., Havukainen, J., Uusitalo, V., Havukainen, M., Soukka, R., Luoranen, M., 2016. Carbon footprint of biobutanol by ABE fermentation from corn and sugarcane. Renew. Energy 89, 401–410. https://doi.org/10.1016/j.renene.2015.12.016

Wu, X., Fang, G., Tong, Y., Jiang, D., Liang, Z., Leng, W., Liu, L., Tu, P., Wang, H., Ni, J., Li, X., 2018. Catalytic Upgrading of Ethanol to n-Butanol: Progress in Catalyst Development. ChemSusChem 11, 71–85. https://doi.org/10.1002/cssc.201701590

Yang, C., Meng, Z., 1993. Bimolecular condensation of ethanol to 1-butanol catalyzed by alkali cation zeolites. J. Catal. 142, 37–44. https://doi.org/10.1006/jcat.1993.1187

Yoshioka, T., Tsuchida, T., Kubo, J., Sakuma, S., 2015. Method for producing alcohol by Guerbet reaction. US 9,056,811 B2.

Figure Captions

Figure 1. Guerbet reaction pathways of ethanol to higher alcohols.

Figure 2. Continuous flow reactor for ethanol conversion. (a - stainless steel rods; b - SiC packing for feed preheating; c - catalyst bed; d - thermowell; e - oil jacket)

Figure 3. Process concept for the four base cases of ethanol conversion to butanol and higher alcohols. The values of reboiler, condenser and heat exchanger duties are for Case 35L.

Figure 4. Residue curve map for ethanol/n-butanol/water system at 5.0 bar absolute (Aspen Plus V8.4 SR-Polar equation of state). Dashed lines represent material balances for distillation columns TC1 (S8-S2-S3) and TC3 (S6-S3-S7) for Cases 35L and 70H with feed and product streams excluding light byproducts such that S3=S5. ■ – n-butanol/water binary azeotrope; ◆ – ethanol/water binary azeotrope. Distillation boundary is the curved solid line between azeotropes.

Figure 5. Required n-butanol selling price vs. ROI for four base cases in Table 3.

Figure 1.

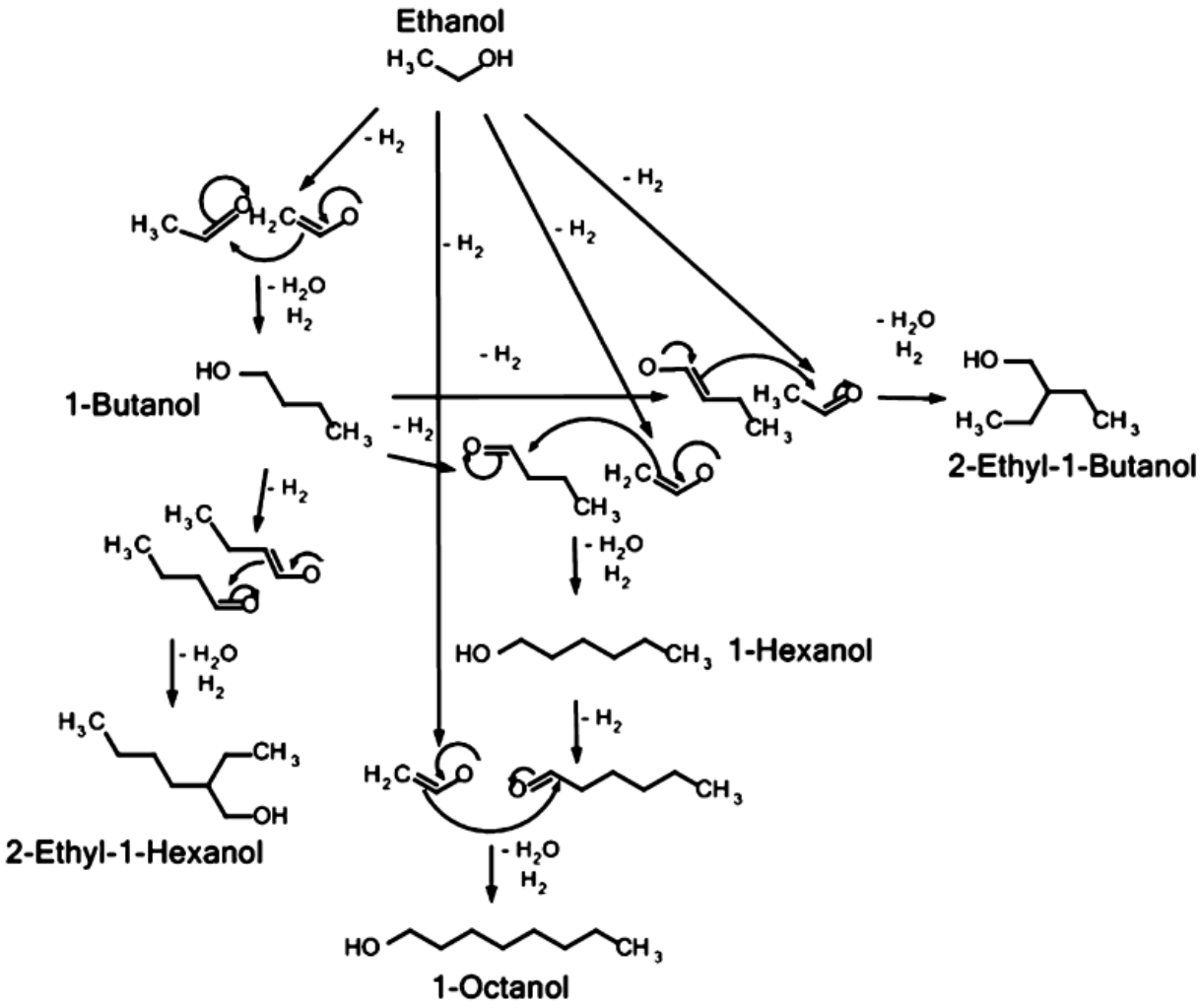
Ethanol
- H2
- H2
- H2
- H2
- H2O
H2
1-Butanol
- H2
- H2O
H2
2-Ethyl-1-Butanol
- H2
- H2O
H2
1-Hexanol
- H2O
H2
2-Ethyl-1-Hexanol
- H2
- H2O
H2
1-Octanol

Figure 2.

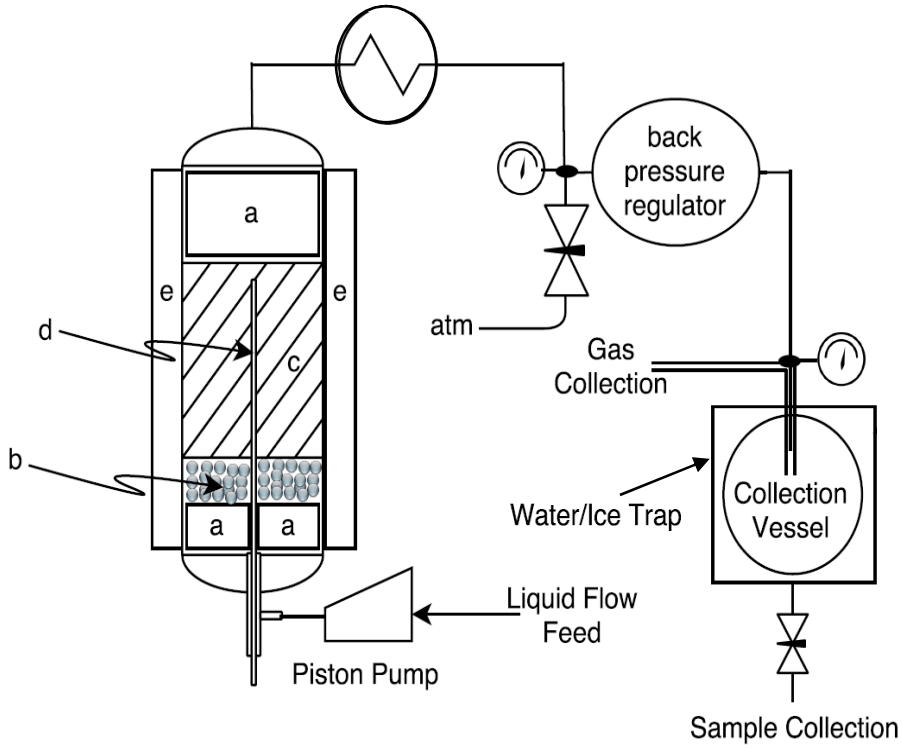
back
pressure
regulator
a
e
e
d
c
b
a
a
atm
Gas
Collection
Collection
Vessel
Water/Ice Trap
Liquid Flow
Feed
Piston Pump
Sample Collection

Figure 3.

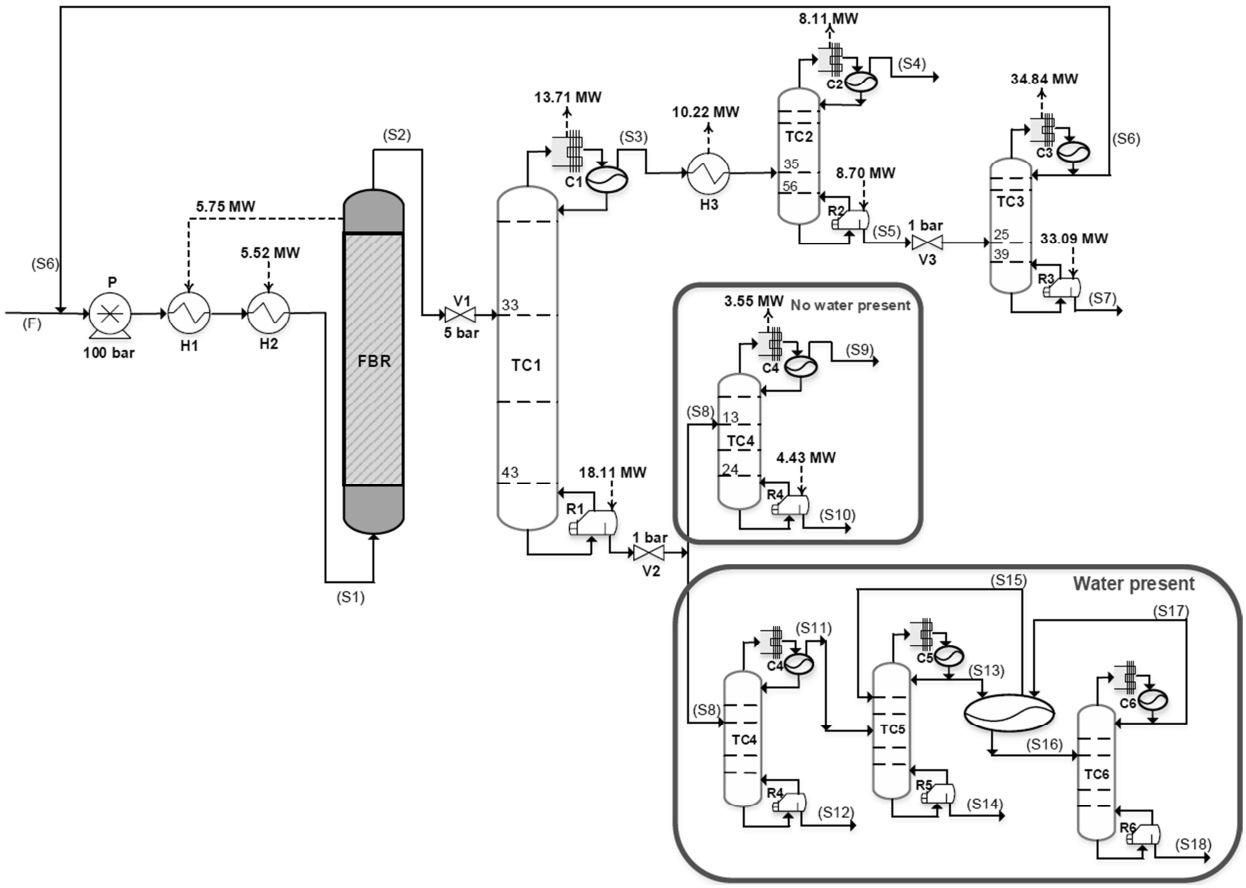
8.11 MW
C2
(S4)
34.84 MW
C3
(S6)
13.71 MW
C1
(S3)
10.22 MW
H3
TC2
35
56
8.70 MW
R2
(S5)
1 bar
V3
TC3
25
39
33.09 MW
R3
(S7)
(S2)
5.75 MW
5.52 MW
(S6)
P
(Γ)
100 bar
H1
H2
FBR
V1
5 bar
TC1
33
43
18.11 MW
R1
1 bar
V2
(S1)
3.55 MW
No water present
C4
(S9)
(S8)
13
TC4
24
4.43 MW
R4
(S10)
Water present
(S15)
(S17)
(S11)
C4
C5
(S13)
C6
(S8)
TC4
TC5
(S16)
TC6
R4
(S12)
R5
(S14)
R6
(S18)

Figure 4.

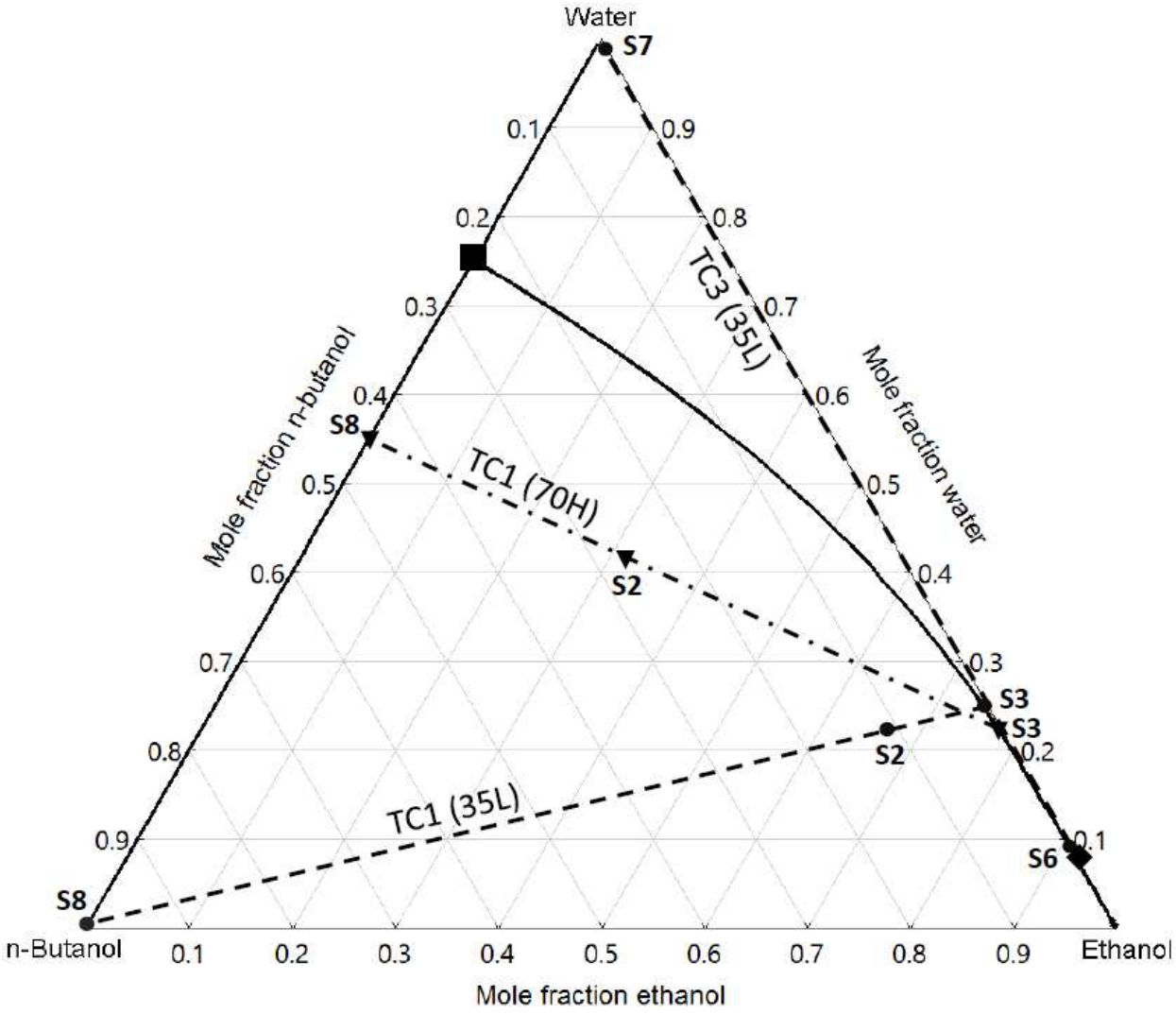
Water
S7
0.1
0.9
0.2
0.8
TC3 (35L)
0.3
0.7
Mole fraction water
0.4
0.6
S8
Mole fraction n-butanol
TC1 (70H)
0.5
0.5
0.6
0.4
S2
0.7
0.3
S3
S3
0.8
S2
0.2
TC1 (35L)
0.9
0.1
S6
S8
n-Butanol
0.1
0.2
0.3
0.4
0.5
0.6
0.7
0.8
0.9
Ethanol
Mole fraction ethanol

Figure 5.

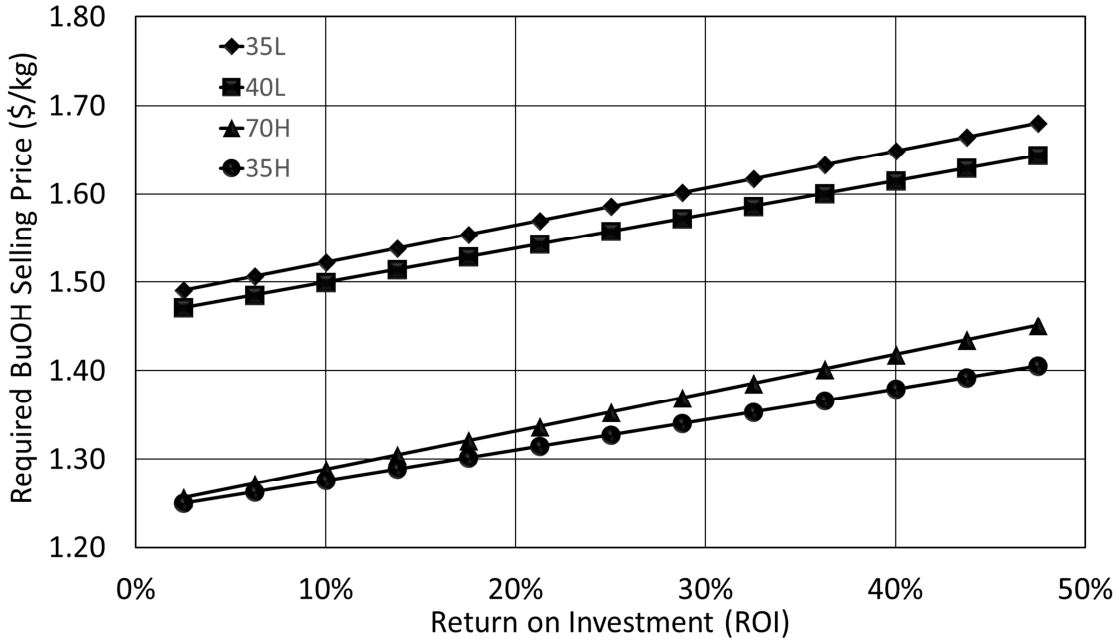
1.80
1.70
1.60
1.50
1.40
1.30
1.20
Required BuOH Selling Price ($/kg)
35L
40L
70H
35H
0%
10%
20%
30%
40%
50%
Return on Investment (ROI)

Continuous Condensed-Phase Ethanol Conversion to Higher Alcohols: Experimental Results and Techno-Economic Analysis

Iman Nezam, Lars Peereboom, and Dennis J. Miller
Department of Chemical Engineering and Materials Science
Michigan State University
East Lansing, Michigan 48824

SUPPLEMENTARY INFORMATION

Table S1. Selectivities of all products formed in selected fixed bed reactor experiments.

Catalyst	1 wt% Ni/9 wt% La_2O_3/γ-Al_2O_3							8 wt% Ni/4.5 wt% La_2O_3/γ-Al_2O_3				
Temp.(^oC)	210	230	230	230	250	250	250	210	210	210	210	230
WHSV (h^{-1})	1.4	0.8	1.4	2.1	0.8	1.4	2.1	0.8	1.1	1.4	1.8	1.4
Conversion	7.0%	22.4%	14.9%	12.0%	41.1%	28.9%	23.2%	29.0%	25.8%	21.9%	21.7%	42.3%
	Selectivities											
n-Butanol	68.0%	58.2%	61.6%	62.9%	50.9%	54.4%	58.1%	59.2%	57.3%	57.9%	56.2%	45.5%
1-Hexanol	7.2%	11.9%	10.8%	9.5%	12.9%	12.3%	3.6%	8.5%	8.2%	8.1%	8.2%	7.9%
2-Ethyl-1-Butanol	2.1%	4.6%	3.4%	2.7%	5.3%	4.2%	3.5%	3.8%	3.3%	3.1%	3.0%	3.4%
1-Octanol	0.7%	2.7%	2.1%	1.6%	3.5%	3.1%	2.4%	1.0%	1.0%	1.0%	1.0%	1.2%
2-Ethyl-1-Hexanol	0.3%	1.3%	0.9%	0.6%	1.7%	1.3%	0.9%	0.7%	0.6%	0.6%	0.6%	0.7%
Diethyl Ether	1.0%	0.8%	0.9%	1.0%	0.8%	0.8%	0.9%	1.8%	1.7%	1.4%	1.5%	0.5%
Acetaldehyde	2.2%	1.6%	2.0%	2.3%	1.2%	1.6%	1.9%	2.9%	3.0%	6.2%	3.6%	5.3%
Butyraldehyde	0.3%	0.7%	0.7%	0.7%	0.9%	1.0%	1.1%	0.6%	0.7%	1.8%	1.0%	2.5%
Ethyl Acetate	0.0%	0.9%	1.0%	1.0%	1.1%	1.2%	1.3%	2.2%	2.0%	2.8%	1.8%	0.5%
Acetal	6.0%	1.1%	1.9%	2.7%	0.5%	0.8%	1.2%	0.9%	1.2%	0.0%	1.8%	0.0%
Unidentified Liquids	6.2%	4.7%	4.4%	4.6%	4.8%	5.3%	5.2%	2.1%	1.9%	1.0%	1.4%	0.6%
Carbon Monoxide	0.1%	0.2%	0.2%	0.2%	0.2%	0.2%	0.1%	0.6%	0.4%	0.3%	0.1%	0.6%
Carbon Dioxide	0.2%	1.3%	0.8%	0.7%	2.6%	1.9%	5.2%	3.6%	2.6%	2.0%	1.7%	5.3%
Methane	4.6%	6.0%	5.8%	5.7%	8.0%	7.3%	4.2%	14.5%	12.1%	11.6%	10.8%	17.8%
Ethane	0.2%	0.7%	0.5%	0.4%	0.8%	0.7%	0.7%	0.9%	0.8%	0.7%	1.1%	1.2%
Propane	0.2%	1.3%	0.8%	0.7%	3.1%	2.3%	1.0%	2.4%	1.7%	1.3%	1.7%	3.6%
Sum	99.3%	98.0%	97.7%	97.3%	98.1%	98.4%	91.3%	105.5%	98.4%	99.7%	95.4%	96.5%

Formulas for Cost Estimation

The following section contains the formulas used in the estimation of equipment purchase costs for the proposed process. Where identical, the definition of various symbols is not repeated after each equation.

1. Reactor (Shell and tube configuration) (Purohit, 1983)

$$C_R\ (\$) = b[(1 + C_T)A]E_i$$

where

$$b\ (base\ cost, \$/ft^2) = \left[\frac{6.6}{1-e^{\left[\frac{7-D_i}{27}\right]}}\right] pfr$$

D_i (in)= shell I.D.

p= cost multiplier for O.D., pitch and layout angle= 0.98

f= cost multiplier for TEMA-type front head= 0.95

r= cost multiplier for TEMA-type rear head= 0.9

C_T= sum of base cost corrections for shell type, expansion joint, tube length, number of tube passes, shell side and tube side design pressures, materials of construction, and tube gage= 2.3

A (ft^2) = surface area for heat transfer

E_i = escalation index (Chemical Engineering Plant Cost Index) (Economic Indicators, 2017)

2. Tray column (Couper et al., 2005)

$$C_{TC}(\$) = (f_1 C_{bs} + N f_2 f_3 f_4 C_{bt} + C_{pl})E_i$$

where

$$C_{bs} = \ base\ shell\ cost\ (\$) = \exp[7.12 + 0.148(lnW) + 0.0249(lnW)^2 + 0.0158\left(\frac{L}{D}\right)\ln(\frac{T_b}{T_p})$$

$$C_{bt} = \ base\ tray\ cost\ (\$) = 375.5\exp(0.1379D)$$

$$C_{pl} = \ base\ platforms\ and\ ladders\ cost\ (\$) = 204.9D^{0.6332}L^{0.8016}$$

f_1= cost multiplier for column material= 2.1

f_2= cost multiplier for column material= 1.7

f_3= cost multiplier for tray type= 0.95

f_4= cost multiplier for tray numbers= 0.1-1.5

N= number of trays

W (lb)= vessel weight

L (ft)= column height

D (ft)= column diameter

T_b (in)= head thickness

T_p (in)= shell thickness

3. Steam generator (Peters et al., 2003)

$$C_{SG}(\$) = C_{bg}E_i$$

where

C_{bg} ($)= base steam generator cost

4. Air cooled heat exchanger (Process Engineering Guide : Air Cooled Heat Exchanger Design, n.d.)

$$C_C(\$) = C_{ac}SE_i$$

where

$S = reduced\ heat\ load\ (kW/°C) = Q/(T_i - T_a\ )$

C_{ac} (^oC $/kW)= cost function= 5-11 (process inlet and outlet temperature dependent)

T_i (^oC)= process inlet temperature

*T_a (^oC)= ambient temperature= 40 ^oC (*Except for one heat exchanger in the ethylene glycol case where $T_a = 30\ ^oC$)*

Q (kW)= heat load

5. Other heat exchangers (Fraas, 1989)

$$C_{HE}(\$) = C_B F_D F_P F_M E_i$$

where

$C_B\ = base\ cost\ (\$) = \exp[8.551 - 0.30863(lnA) + 0.06811(lnA)^2]$

A (ft^2)= Exchanger surface area

F_D= cost multiplier for the exchanger type = 0.7 for fixed head and 1.4 for kettle reboiler

F_P= cost multiplier for the design-pressure (surface area dependent)

F_M= cost multiplier for the material of construction (surface area dependent)

Table S2. Specifications of reactor and distillation columns for four base case scenarios

CASE[a]	**35L**	**40L**	**35H**	**70H**
Reactor (100 bar, 230 ^{o}C)				
Number of tubes (1" 20 BWG)	5144	5144	5144	8117
Tube length (m)	16.5	17.8	16.5	18.8
Catalyst mass (10^4 kg)	3.60	3.93	3.60	6.56
WHSV (kg EtOH/kg catalyst/h)	1.45	1.15	1.45	0.33
Cost (10^3 $)	2,350	2,580	2,350	4,500
Column 1 (TC1) (5 bar absolute pressure)				
Number of actual stages	44	45	49	67
Feed stage	33	28	33	21
Diameter (m)	3.0	2.8	2.7	1.5
Reflux ratio (L_o/D)	1.2	1.2	1.5	3.0
Boilup ratio (V_N/B)	12.7	11.2	10.8	3.2
Cost (10^3 $)	670	670	630	380
Column 2 (TC2) (5 bar absolute pressure)				
Number of actual stages	57	47	57	49
Feed stage	35	33	23	40
Diameter (m)	1.7	1.6	1.2	0.6
Reflux ratio	4.5	4.5	6.8	3.5
Boilup Ratio	0.9	1.0	0.5	0.6
Cost (10^3 $)	370	330	270	140
Column 3 (TC3) (1 bar absolute pressure)				
Number of actual stages	40	44	50	55
Feed stage	25	28	35	16
Diameter (m)	4.2	3.5	3.5	1.9
Reflux ratio	3.0	2.5	2.5	3.5
Boilup ratio	16.8	11.7	12.5	22.7
Cost (10^3 $)	1,110	850	920	420
Column 4 (TC4) (1 bar absolute pressure)				
Number of actual stages	25	25	25	25
Feed stage	13	11	13	13
Diameter (m)	1.9	1.9	1.9	2.7
Reflux ratio	2.5	2.5	2.5	2.0
Boilup ratio	16.6	16.6	14.4	29.1
Cost (10^3 $)	290	390	280	460
Column 5 (TC5) (1 bar absolute pressure)				
Number of actual stages	-	-	-	12
Feed stage	-	-	-	11
Diameter (m)	-	-	-	2.4
Reflux ratio	-	-	-	2.5
Boilup ratio	-	-	-	6.2
Cost (10^3 $)	-	-	-	280
Column 6 (TC6) (1 bar absolute pressure)				
Number of actual stages	-	-	-	20

Feed stage	-	-	-	6
Diameter (m)	-	-	-	2.0
Reflux ratio	-	-	-	1.5
Boilup ratio	-	-	-	7.4
Cost (10^3 $)	-	-	-	270
Steam Generator (45 bar, 257 ^oC)				
Capacity (10^3 kg/h)	97.4	80.3	67.9	61.0
Cost (10^3 $)	1,520	1,240	1,050	970

[a]Case designations: The number refers to per-pass ethanol conversion in the fixed-bed reactor; "L" refers to low selectivities of 60% to n-butanol, 16% to C_6+ alcohols; "H" refers to high selectivities of 72% to n-butanol and 22% to C_6+ alcohols.

Table S3. Parameters for heat exchangers for Case 35L.

Unit	Target T (^oC)	Approach ΔT (^oC)	Heat Duty[a,b] (MW)	Area (m^2)	Cost (10^3 $)	Function
H1	177	53	5.8	68	60	Feed preheat using steam from reactor
H2	230	27	5.5	133	80	Feed preheat using generated steam
H3	95	55	-10.2	1330	160	Cooler between TC1 and TC2
C1	122	82	-13.7	218	180	Partial condenser on column TC1
R1	176	81	18.1	263	310	Partial reboiler on column TC1
C2	57	17	-8.1	619	520	Partial condenser on column TC2
R2	126	130	8.7	78	120	Partial reboiler on column TC2
C3	78	38	-34.8	1180	980	Total condenser on column TC3
R3	99	158	33.1	246	290	Partial reboiler on column TC3
C4	118	78	-3.6	59	50	Total condenser on column TC4
R4	152	105	4.4	50	80	Partial reboiler on column TC4

[a]All process heat provided by steam (257 ^oC, 45 bar) from steam generator except for Heater 1.

[b]All process cooling provided by direct air cooling in forced convection air-cooled heat exchangers. The area reported for air-cooled heat exchangers is bare tube area; fin:tube area ratio = 17:1.

Table S4. Composition of Process Streams for 35L Case

Stream	F	S1	S2	S3	S4	S5	S6	S7	S8	S9	S10
Temperature (^oC)	25.0	230.0	210.0	121.9	57.2	126.5	78.5	98.9	122.1	117.9	151.8
Pressure (bar)	1.0	100.0	100.0	5.0	5.0	5.0	1.0	1.0	5.0	1.0	1.0
	Mole Flows (kmol/h)										
Ethanol	402.8	1124.3	730.7	730.6	9.0	721.6	721.5	0.1	0.1	0.1	0.0
n-Butanol	0.0	0.0	118.0	0.1	0.0	0.1	0.0	0.1	117.9	117.8	0.1
1-Hexanol	0.0	0.0	10.5	0.0	0.0	0.0	0.0	0.0	10.5	0.0	10.5
2-Ethyl-1-Butanol	0.0	0.0	10.5	0.0	0.0	0.0	0.0	0.0	10.5	0.1	10.4
Water	0.0	70.4	242.5	242.5	1.0	241.5	70.4	171.1	0.0	0.0	0.0
Carbon Dioxide	0.0	0.0	29.5	29.5	29.5	0.0	0.0	0.0	0.0	0.0	0.0
Methane	0.0	0.0	99.6	99.6	99.6	0.0	0.0	0.0	0.0	0.0	0.0
Diethyl Ether	0.0	0.0	6.5	6.5	6.5	0.0	0.0	0.0	0.0	0.0	0.0
Ethyl Acetate	0.0	1.1	9.5	9.5	8.4	1.1	1.1	0.0	0.0	0.0	0.0
Hydrogen	0.0	0.0	6.0	6.0	6.0	0.0	0.0	0.0	0.0	0.0	0.0
Total	402.8	1195.8	1263.3	1124.3	160.0	964.3	792.9	171.3	139.0	118.0	21.0

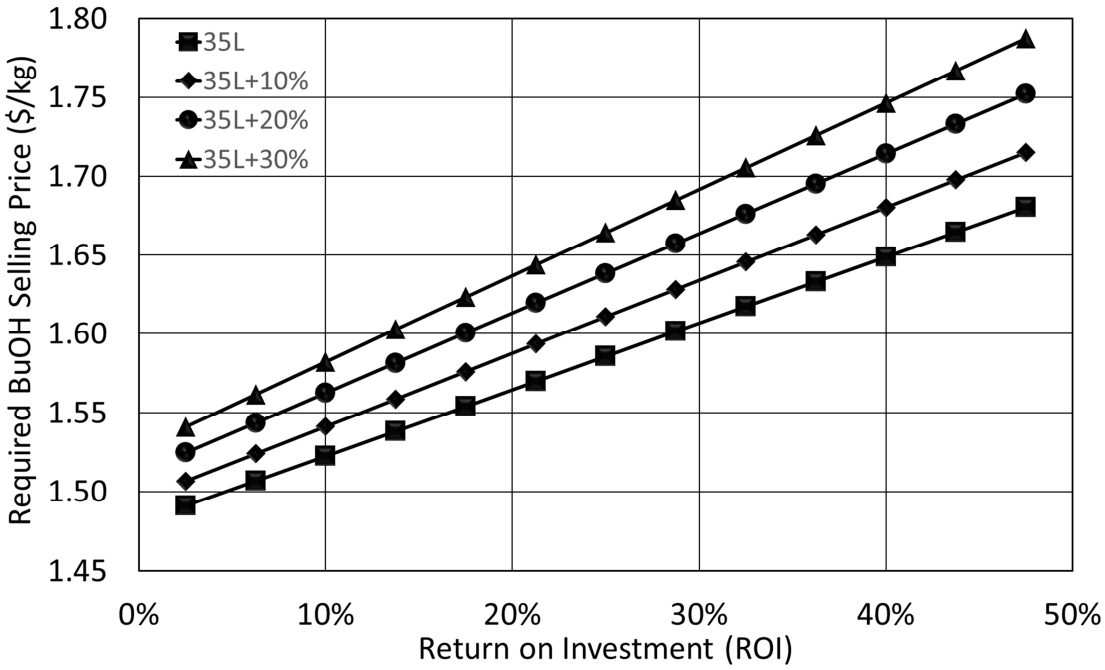

Figure S1. Sensitivity analysis of required n-butanol selling price dependence on purchase equipment costs for Case 35L. Percentage in legend refers to increment in equipment purchase costs over Case 35L equipment purchase costs of $9.14 million.

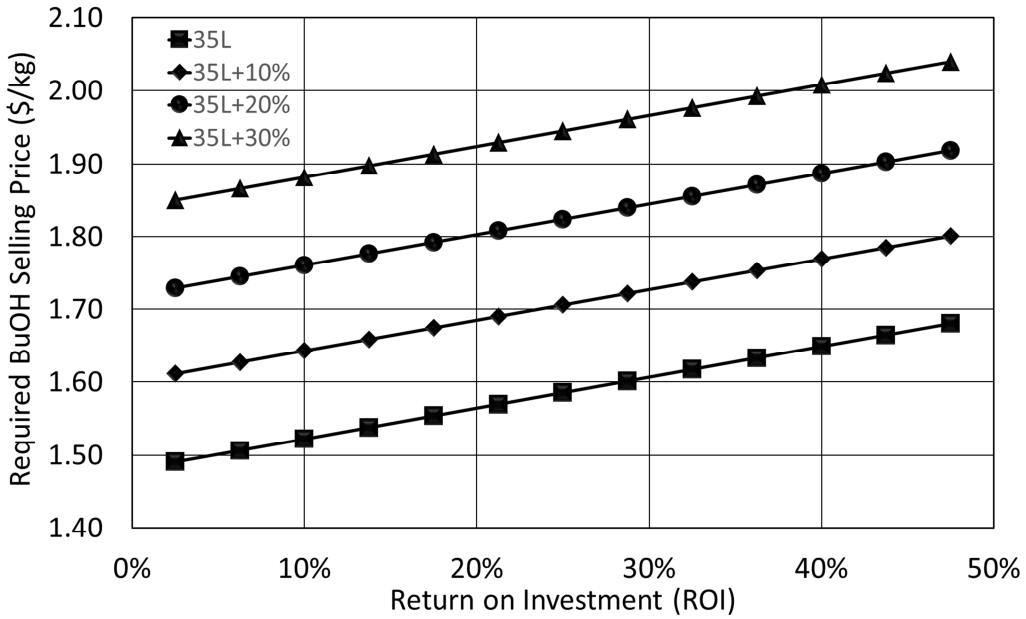

Figure S2. Sensitivity analysis of required n-butanol selling price dependence on ethanol feed cost for Case 35L. Percentage in legend refers to increment in ethanol feed cost relative to Case 35L cost of $1.65/gallon ($0.53/kg).

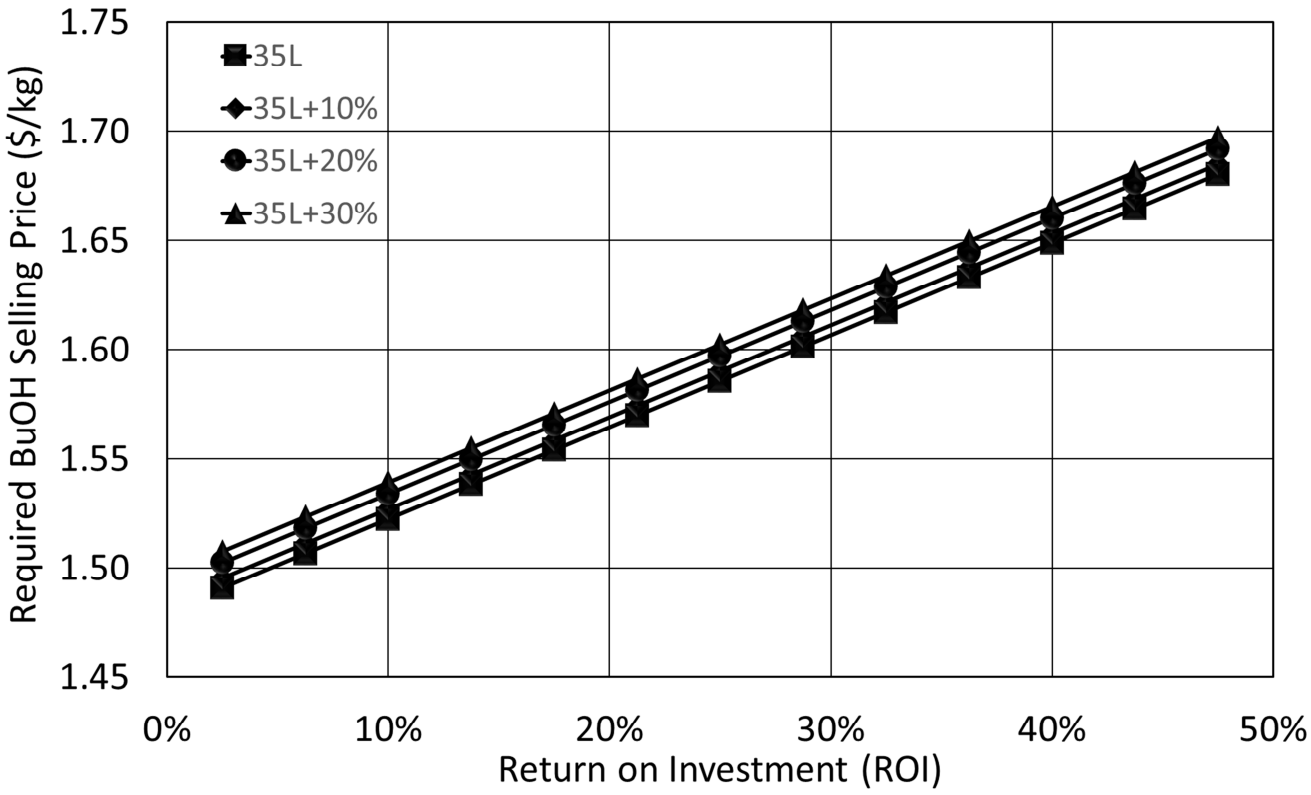

Figure S3. Sensitivity analysis of n-butanol required selling price dependence on utility costs for Case 35L. Percentage in legend refers to increment in total annual utility costs relative to Case 35L utility costs of $5.1 million.